Program Digest, 2019 IEEE International Ultrasonics Symposium (IUS)
Glasgow, Scotland, October 6-9, 2019

Low-cost monolithic processing of large-area ultrasound transducer arrays

L. C. J. M. Peters
Holst Centre
TNO
Eindhoven, the Netherlands
laurens.peters@tno.nl

R. Ollearo
Applied Physics, Molecular Materials and Nanosystems
Eindhoven University of Technology
Eindhoven, the Netherlands
r.ollearo@tue.nl

R. G. F. A. Verbeek
Holst Centre
TNO
Eindhoven, the Netherlands
roy.verbeek@tno.nl

J. L. P. J. van der Steen
Holst Centre
TNO
Eindhoven, the Netherlands
jan-laurens.vandersteen@tno.nl

H. B. Akkerman
Holst Centre
TNO
Eindhoven, the Netherlands
hylke.akkerman@tno.nl

A. W. F. Volker
Department of Acoustics and Sonar
TNO
the Hague, the Netherlands
arno.volker@tno.nl

P. L. M. J. van Neer
Department of Acoustics and Sonar
TNO
the Hague, the Netherlands
paul.vanneer@tno.nl

G. H. Gelinck
Holst Centre
TNO
Eindhoven, the Netherlands
gerwin.gelinck@tno.nl

***Abstract*—Large-area flexible ultrasound arrays can offer new ultrasound modalities in multiple fields. The production of these arrays when using CMOS-type fabrication techniques faces scalability challenges and costs increase dramatically when upscaled to large dimensions. We investigate the monolithic production of large-area PPT (Printed Polymer Transducer) arrays directly on a flexible substrate. Here, a vibrating membrane is defined by a circular opening in a thick photoresist layer. Since the photoresist layer is processed on top of the P(VDF-TrFE), a thin barrier layer is used to prevent diffusion into the P(VDF-TrFE). An annealing procedure is developed to reduce the surface roughness of the P(VDF-TrFE) layer and make it compatible with thin film electrode deposition. We measure a remnant polarization of 7-8 μC/cm^2 and a coercive field of around 50 MV/m. Laser scanning vibrometer measurements reveal a uniform peak displacement and fundamental resonance frequency (66 kHz) across the PPT array.**

***Keywords*—large-area, flexible, ultrasound transducer**

I. Introduction

Large-area ultrasound arrays can enable new modalities in several fields of interest. In the automotive domain, large arrays can offer mid-air haptic feedback with greater intensity and spatial distribution of controls such that the driver does not need to move from the driving position to control the dashboard. In the medical domain, a more accurate diagnosis can be made by offering a larger field of view [1], a reduced result-dependency of the operator can be achieved, [2] and it enables new applications such as photoacoustic imaging [3] and through transmission measurements [4]. In both applications areas, large-area arrays are inherently linked to transducer flexibility since large and completely flat surfaces are uncommon in both car dashboards as well as the human body.

Both the aspect of large-area and flexibility give rise to integration challenges. Currently the majority of transducers are either inherently rigid (ceramics) or processed on a rigid wafer with CMOS technology (CMUT and PMUT). To create flexible arrays, micromachined transducers are either transferred to a flexible substrate (e.g. [5, 6] or the substrate itself is made flexible by either thinning it down [7] or creating trenches [8,9]. In both approaches large-area arrays are challenging, since transfer processes are time-consuming and can cause yield problems, while the (thinned or trenched) silicon substrates have limited flexibility.

As a scalable alternative for producing large-area flexible arrays, we employ monolithically printed transducers directly on a polymer substrate. The transducers are fabricated using thin-film technology, with processes (e.g. coating techniques, photolithography) conventionally used in the flat panel display industry for the mass production of, for example, OLED displays. This ensures scalability, low cost of fabrication, and a route to fast deployment. We have reported the acoustic feasibility of a low-frequency transducer aimed at mid-air haptic feedback last year. Here, we investigate their fabrication methodology, processing challenges and performance.

II. Experimental

A. Transducer fabrication

The PPTs are monolithically fabricated on top of a thin polyimide substrate of a rigid glass carrier. The bottom electrodes are structured using photolithography, after which a structured 20 μm P(VDF-TrFE) layer is stencil-printed on top. After evaporation of an interlayer, a thick photoresist is spin-coated on top. The vibrating membrane is defined by an opening in the thick photoresist layer. The interlayer is dry etched to reveal the piezoelectric layer and a top electrode is thermally evaporated through a shadow mask. After processing the transducers are released (laser assisted or mechanically) from the glass carrier, yielding fully flexible devices with a total thickness of <200 µm.

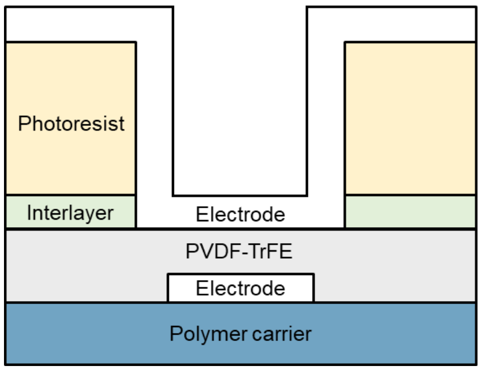

Fig. 1. Shematic of a single single transducer layer stack.

B. Layer analysis

The layer thickness and roughness of the layers were determined using a Veeco Dektak 80. The peak-to-peak roughness of the film was determined as the difference between the highest and the lowest point in the roughness, recorded within a given evaluation length.

C. Electrical characterization

Impedance, resistance and capacitance of the transducers were determined using an Agilent E4980A precision LCR meter. Hysteresis loops were recorded using an AixACCT TF Analyzer 2000.

D. Vibrational characterization

Out-of-plane surface displacement was measured using a laser scanning vibrometer setup, while exiting the PPTs with a linear chirp signals trough a waveform generator. Both the displacement and the natural resonance frequency of the membranes are determined. For an extended description of the setup the reader is referred to [10].

III. Results and Discussion

The membrane radial mode resonance frequency depends on the radius of the opening diameter (a), the membrane thickness (h), Youngs modulus (E) and the Poisson ratio (v), and can be approximated by:

$$f_n = \frac{\lambda_n^2 h}{2\pi a^2}\sqrt{\frac{E}{12\rho(1-v^2)}}$$

with λ a constant depending on the harmonic n, and ρ the membrane density [11]. Currently, the majority of MUTs are being fabricated trough etching (front or back side) of SOI wafers to create the (vibrating) membranes. The membrane itself is therefore commonly made of silicon. Considering that silicon has a Youngs modulus that is 2-3 orders of magnitude higher than common polymeric materials, our polymeric transducer has been created using the relatively thick polymeric carrier as part of the membrane to compensate for the decrease in stiffness (and resulting drop in natural resonance frequency). In addition, the center frequency of the natural resonance is controlled by varying the opening diameter, *a*. In our polymeric transducer, the diameter is defined by an opening in the top photoresist layer. To prevent excessive damping of the membrane vibration, we deposit a relatively thick layer of photoresist (>100 micron), to generate enough stiffness and thereby controlling the transducer's bandwidth.

A. Photoresist processing

Upon processing the photoresist layer on the P(VDF-TrFE) layer, we observed changing electrical characteristics in the piezoelectric layer. LCR measurements before and after the deposition of photoresist show a change in loss factor and a decreased dielectric constant (figure 2). Recorded hysteresis curves show that without the photoresist layer a remnant polarization of 7-8 µC/cm^2 and a coercive field of around 50 MV/m are present. These values are comparable with literature [12]. However, as shown in figure 3, the photoresist layer strongly influences the hysteresis curves. Photoresists commonly contain organic solvents, in this case cyclopentanone. Partial dissolving of P(VDF-TrFE) can lead to diffusion between the two layers resulting in altered electrical behavior. To prevent the layer diffusion, we introduced a thin inorganic interlayer on the P(VDF-TrFE) before spin-coating the photoresist on top. In both the LCR and hysteresis measurement, we observed that this resulted in recovered (piezo)electrical characteristics.

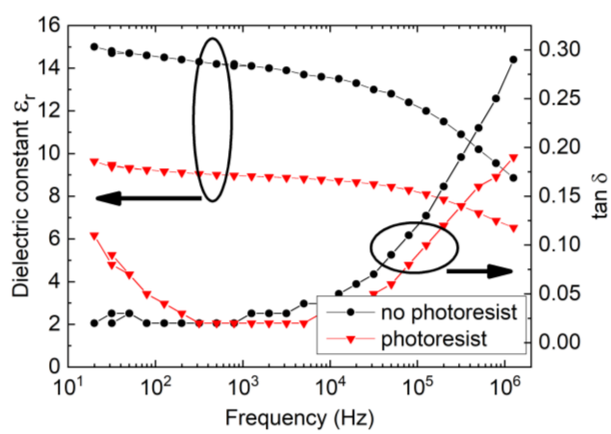

Fig. 2. Dielectric constant, ε_r, and dielectric loss, tan δ, as a function of frequency, of a single PPT measured both before and after depositing photoresist on the piezoelectric layer.

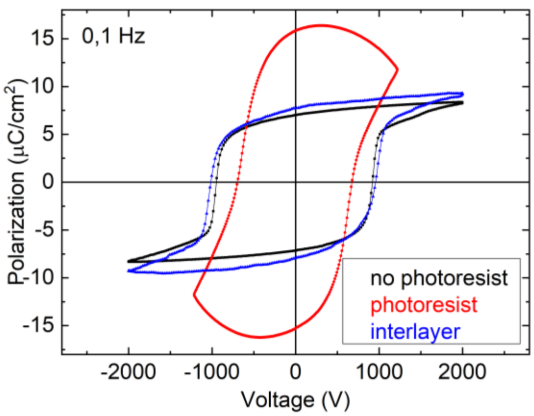

Fig. 3. Recorded hysteresis curves of the piezo of a single PPT at 0.1 Hz, measured withouth photoresist, with photoresist and with the photoresist separated by an interlayer.

B. Surface roughness

The top contact is evaporated directly on the P(VDF-TrFE) surface. Typically in thin-film devices the electrode tracks have a thickness in the order of a hundred nanometer. We found that the P(VDF-TrFE) solution processing steps resulted in a surface roughness of over 1500 nm (peak-to-peak) when processing layers >20 µm (figure 4, black trace), an order of magnitude higher than the electrode thickness. The mismatch can lead to insufficient step-coverage and local amplifications of the electric field, which can in turn lead to dielectric breakdown when poling the piezoelectric layer at high voltages. In addition, the roughness of the P(VDF-TrFE) also partly determines its transparency. A highly transparent piezoelectric is favored for alignment purposes during processing and enables the fabrication of transparent transducers (e.g. for photoacoustic imaging).

It is well reported that a P(VDF-TrFE) layer undergoes structural changes upon annealing [e.g. 13]. SEM images show that during this process the microstructure of the material changes from microporous to microfibrillar. In addition, Li et al. have shown that vapor induced phase separation (VIPS) occurs in presence of water vapor and causes a porous and rough surface to form [14]. This latter work inspired us to investigate the annealing of thick P(VDF-TrFE) layers in vacuum, to eliminate the VIPS effect. In initial experiments, we performed a 30 minute annealing at 130 ºC in air both and vacuum. This temperature has been chosen to obtain maximal piezoelectric response [15]. Both conditions resulted in a similar surface roughness of over 1500 nm peak-to-peak (figure 4, blue trace). Repeating this experiment at 80 ºC however, resulted in a much lower roughness of below 200 nm peak-to-peak. Here, the solvent evaporation (TEP) is considerably slower. Since we need higher temperatures to obtain the desired piezoelectric properties, we attempted a two-step approach of 30 minutes at 80 ºC followed by 30 minutes at 130 ºC (figure 4, red trace). We obtained a low roughness of 200 nm peak-to-peak while maintaining the piezoelectric properties, which is a significant improvement in roughness over the direct annealing methods.

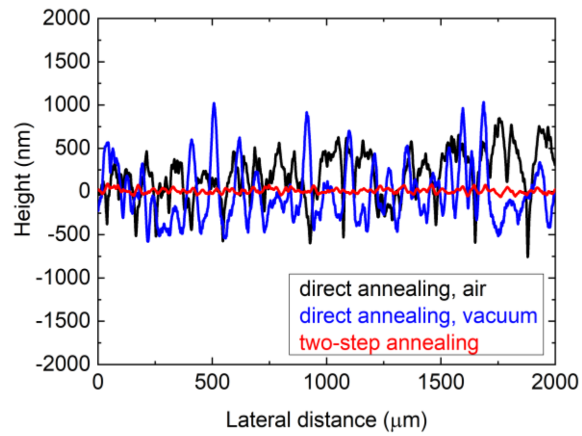

Fig. 4. Recorded hysteresis curves of the piezo of a single PPT at 0.1 Hz, measured withouth photoresist, with photoresist and with the photoresist separated by an interlayer.

C. Accoustic performance

To characterize the membrane performance in arrays, we have fabricated an annular array consisting of 300+ PPTs. The out-of-plane surface displacement of this array was measured using a laser scanning vibrometer setup (figure 5). Apart from two diverging regions (top-right and bottom, caused by local delamination), we obtain a uniform membrane peak displacement of on average 242 nm. In addition, we determined the fundamental resonance of all membranes (figure 6). Apart from a few outliers, the majority of elements has its fundamental resonance frequency around 66 kHz. For an extended description of these measurements and in-air accoustic measurements, the reader is referred to [10, 16].

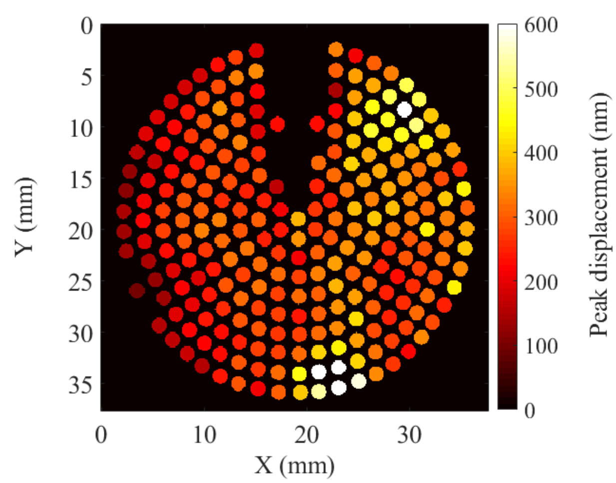

Fig. 5. Measured peak out-of-plane displacement across a 300+ element PPT annular array. The average peak displacement is 242 nm. Two deverging regions (top right an bottom) are attributed to local delamination.

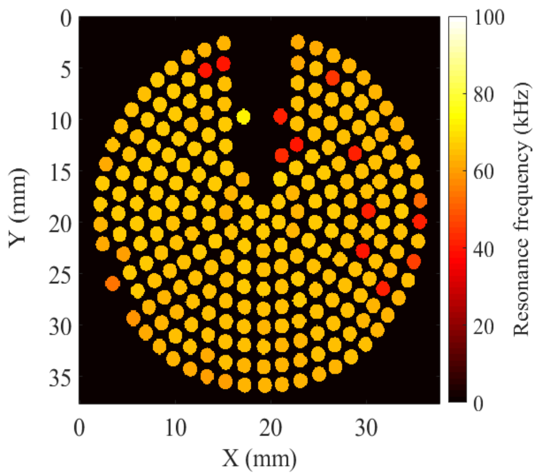

Fig. 6. Measured fundamental resonance frequency of each PPT of a 300+ element annular array. Apart from a few outliers, a uniform resonance frequency of 66 kHz is found across the array.

IV. Conclusion

We demonstrated that we can monolithically fabricate a flexible PPT array, where the flexible membrane is composed of the piezoelectric layer as well as the flexible substrate it is processed on. To make the piezoelectric layer compatible with thin-film processes, we reduced its surface roughness using an adapted annealing procedure and applied a barrier to protect the active layer from solvent diffusion and thereby, preventing piezoelectric performance loss. The piezoelectric layer shows on par remnant polarization values. The PPTs have a natural resonance frequency of 66 kHz and show uniform behavior across the array.

Acknowledgment

This work has been supported by the EU-funded H2020 ECSEL project SILENSE (ID 737487).

References

[1] H. Yerli, S. Y. Eksioglu, "Extended Field-of-View Sonography Evaluation of the Superficial Lesions", Canadian Association of Radiologist Journal, vol 60, pp. 35-39, February 2009.

[2] D. P. Bahner, J. M. Blickendorf, M. Bockbrader, E. Adkins, A. Vira, C. Boulger, A. R. Panchal, "Language of Transducer Manipulation", Journal of Ultrasound in Medicine, vol 35, pp 183-188, January 2016.

[3] Z. Xie, X. Wang, R. F. Morris, F. Padilla, G. LeCarpentier, P. Carson, "Photoacoustic imaging for deep targets in the breast using a multichannel 2D array transducer." Proc. SPIE 7899, Photons Plus Ultrasound: Imaging and Sensing, pp. 789907, April 2011.

[4] D. Lin, R. Wodnicki, X. Zhuang, C. Woychik, K. E. Thomenius, R. A. Fisher, D. M. Mills, A. J. Buyn, W. Burdick, P. Khuri-Yakub, B. Bonitz, T. Davies, G. Thomas, B. Otto, M. Töpper, T. Fritzsch, O. Ehrmann, "Packaging and Modular Assembly of Large-Area and Fine-Pitch 2-D Ultrasnoic Transducer Arrays", IEEE Transactions on Ultrasonics, Ferroelectrics, and Frequency Control, vol 60, pp. 1356-1375, July 2013.

[5] S. Sun, M. Zhang, C. Gao, B. Liu, "Flexible Piezoelectric Micromachined Ultrasonic Transducers Towards New Applications", IEE International Ultrasonics Symposium, October 2018.

[6] C. Wang, X. Li, H. Hu. L. Zhang, Z. Huang, M. Lin, Z. Zhang, Z. Yin, B. Huang, H. Gong, S. Bhaskaran, Y. Gu, M. Makihata, Y. Guo, Y. Lei, Y. Chen, C. Wang, Y. Li, T. Zhang, Z. Chen, A. Pisano, L. Zhang, Q. Zhou, S. Xu, "Monitoring of the central blood pressure waveform via a conformal ultrasonic device", Nat. Biomed. Eng., vol 2, pp. 687-695, September 2018.

[7] K. A. Wong, S. Panda, I. Ladabaum, "Curved micromachined ultrasonic transducer", Porceedings of the IEEE Ultrasnoics Symposium, vol 1, pp. 572-576, November 2003.

[8] X. Zhuang, D. E. Lin, O. Oralkan, P. T. Khuri-Yakub, "Fabrication of Flexible Transducer Arrays With Through-Wafer Electrical Interconnects Based on Trench Refilling With PDMS", Journal of Microelectromechanical Systems, vol 17, pp. 446-452, May 2008.

[9] Y. Huang, "CMUT Packaging for Ultrasound System", United States patent US20100280388A1, November 2010.

[10] P. L. M. J. van Neer, A. W. F. Volker, A. P. Berkhoff, T. Schrama, H. B. Akkerman, A. van Breemen, L. C. J. M Peters, J. L. P. J. van der Steen, G. H. Gelinck, "Development of a flexible large-area array based on printed polymer transducers for mid-air haptic feedback", Proc. ICU Symp., Bruges, Belgium, 2019, *in press*.

[11] R. Bader, Springer Handbook of Systematic Musicology, 1st edition, 2018, pp. 55.

[12] S. Chen, K. Yao, F. E. H. Yayt, L. L. S. Chew, "Comparative investigation of the structure and properties of ferroelectric poly(vinylidene fluoride) and poly(vinylidene fluoride–trifluoroethylene) thin films crystallized on substrates", Journal of Applied Polymer Science, vol 116, pp. 3331-3337, June 2010.

[13] R. I. Mahdi, W. C. Gan, W. H. Abd. Majid, "Hot Plate Annealing at a Low Temperature of a Thin Ferroelectric P(VDF-TrFE) Film with an Improved Crystalline Structure for Sensors and Actuators", vol 14, pp. 19115-19127, September 2014.

[14] M. e. a. Li, "Controlling the microstructure of poly(vinylidene-fluoride) (PVDF) thin films for microelectronics", Journal of Materials Chemistry C, vol. 1, pp. 7695-7702, September 2013.

[15] P. Ducrot, I. Dufour, C. Ayela, "Optimization Of PVDF-TrFE Processing Conditions For The Fabrication Of Organic MEMS Resonators", Scientific Reports, vol 6, pp. 19426, January 2016.

[16] P. L. M. J. van Neer, A. W. F. Volker, A. P. Berkhoff, H. B. Akkerman, T. Schrama, A. van Breemen, G. H. Gelinck, 'Feasiblity of using printed polymer transducers for mid-air haptic feedback', Proc. IEEE Ultrasonics Symp, Kobe, Japan, 2018.